

## Review

# Mafic and ultramafic rocks in parts of the Bhavani complex, Tamil Nadu, Southern India: Geochemistry constraints

Ali Mohammed Dar<sup>1\*</sup>, Akhtar R. Mir<sup>2</sup>, K. Anbarasu<sup>1</sup>, M. Satyanarayanan<sup>3</sup>, V. Balaram<sup>3</sup>,  
D. V. Subba Rao<sup>3</sup> and S. N. Charan<sup>3</sup>

<sup>1</sup>Department of Geology, Periyar University, Salem, Tamilnadu-636011, India.

<sup>2</sup>Department of Earth Science, University of Kashmir, Srinagar-190006, India.

<sup>3</sup>National Geophysical Research Institute, Council of Scientific and Industrial Research, Uppal Road, Hyderabad-500606, India.

Received 9 January, 2014; Accepted 19 February, 2014

Present paper deals with the petrogenesis of gabbros and pyroxenites of Bhavani complex, Tamil Nadu, Southern India. Studied gabbros are mainly composed of pyroxenes with minor plagioclase (An<sub>10-30</sub>) and amphibole minerals. Pyroxenites are composed of coarse-grained clinopyroxenes, orthopyroxenes and medium-grained hornblende minerals. Geochemically, in the total alkali vs. SiO<sub>2</sub> diagram studied samples are broadly classified as gabbros and their magma type is tholeiitic in nature, however, based on the TiO<sub>2</sub>, MnO, P<sub>2</sub>O<sub>5</sub> diagram most of the studied samples fall within the calc-alkaline basaltic (CAB) field. In chondrite-normalized rare earth element (REEs) patterns, pyroxenites show negative Eu anomaly with slight enrichment of heavy rare earth elements (HREEs). The negative Eu anomaly in these samples indicates fractionation of plagioclase. The flat chondrite-normalized REEs pattern of gabbros in association with low CaO, Al<sub>2</sub>O<sub>3</sub>, Sr content and absence of Eu anomaly suggest removal of plagioclase component from basic parental magma. In primitive mantle (PM) and mid-ocean ridge basalt (MORB) normalized incompatible trace element patterns studied samples have enrichment of large ion lithophile elements (LILEs) and light rare earth elements (LREEs). Tectonic setting discrimination diagrams, in addition to their geochemical characteristics such as Nb-Ta, Zr-Hf negative anomalies and low values of (La/Yb)<sub>cn</sub> and (La/Sm)<sub>cn</sub>, suggest volcanic arc tectonic setting.

**Key words:** Bhavani, layered complex, Geochemistry, light rare earth elements (LREEs), large ion lithophile elements (LILEs), petrogenesis.

## INTRODUCTION

The Bhavani ultramafic complex and Sittampundi ultrabasic complex is considered to be age of 2898 ± 50

Ma years arrived at by the Sm-Nd systematics (Bhaskara Rao et al., 1996). According to Bhaskar Rao et al. (1996)

\*Corresponding author. E-mail: mtekali@gmail.com

Author(s) agree that this article remain permanently open access under the terms of the [Creative Commons Attribution License 4.0 International License](https://creativecommons.org/licenses/by/4.0/)

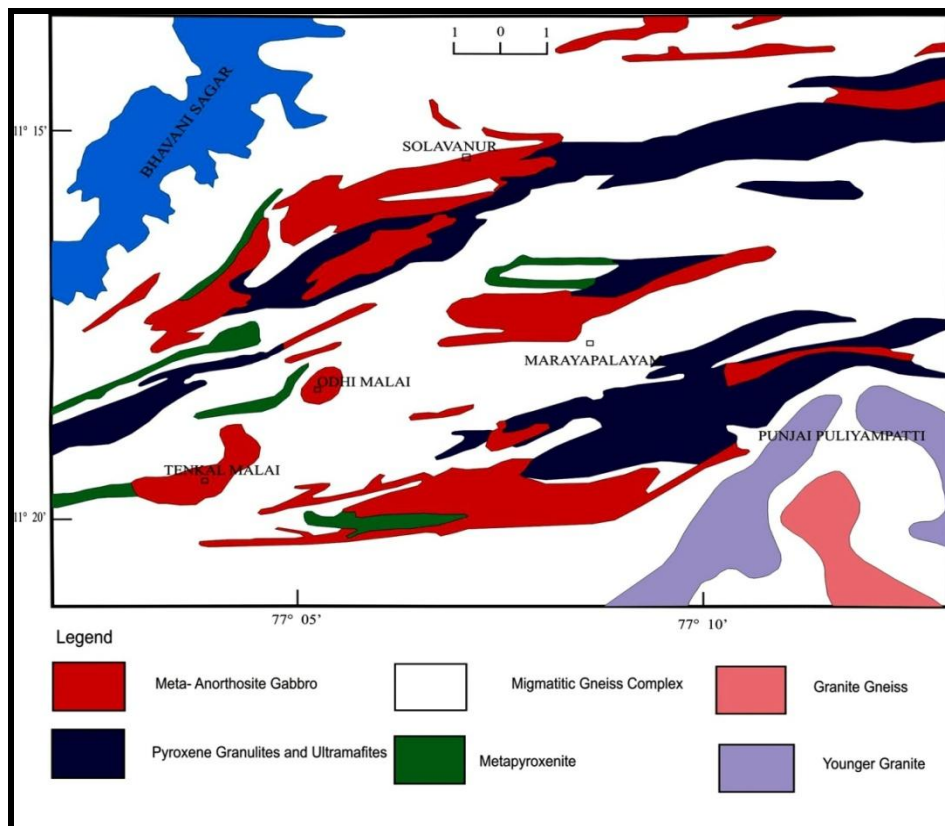


**Figure 1.** Geological map of Bhavani complex showing distribution of E-W trending mafic-ultramafic rocks after Selvan (1981).

the rocks of Bhavani layered complex, was subjected to three phases of deformation. The earliest of these was in the form of tight isoclinal folds with an E-W axis, followed by the second phase of coaxial tight synformal and antiformal folds. These two deformation phases led to the interleaving of the components of the Bhavani Layered Complex with those of Sathyamangalam Group. During the course of the third phase of deformation, there was cross-folding and slicing up of the complex, giving rise to structural domes and basins. Due to intense deformation and mineral segregation, the gabbroic rocks exhibit banded structures with alternating leucocratic and melanocratic bands. A group of ultrabasic rocks ranging in composition from dunite, peridotite, garnetiferous gabbro, gabbroic anorthosite to anorthosite are traced along the Bhavani river valley in the Coimbatore and the Erode districts of Tamil Nadu, South India, forming part of the Bhavani Layered Complex (Selvan, 1981; Subramanian and Selvan, 2001). These bodies are considered to be emplaced in the weak zones of deep-seated fractures in crustal rocks and emplaced into the rocks of the Sathyamangalam Group. There is a dearth of petrological and geochemical data on mafic and ultramafic rocks of the Bhavani Layered Complex. The present paper embodies the results of the petrological

and geochemical analysis of mafic and ultramafic rocks of Odhimalai and Thenkalmalai areas located within the Bhavani Complex (Figure 1). Odhimalai is a bi-symmetrical hillock with an altitude of 654 m above Mean Sea Level (MSL) and elevated about 250 m from the base of the hill. The Thenkalmalai is a linear ridge with an altitude of ~ 389 m above MSL. Both of the hillocks are striking ENE – WSW directions.

## GEOLOGIC SETTING

In Palghat–Cauvery suture zone, dismembered units of Archaean layered complexes comprising calcic-meta anorthosites, websterites, clinopyroxenite, pyroxenite, mafic granulites and serpentinised dunite occur as linear bands for a distance of more than 250 km. from the southern margin of Nilgiri massif to Sittampundi in the east. The detailed field studies of two hillocks (Odhimalai and Thenkalmalai) lead to the recognition of an array of rock types including metagabbro, meta-anorthositic gabbros, pyroxenites, and peridotite, occurring as layers in close association (Rao et al., 1996). The dominant member of both the hillocks is metagabbro and pyroxenite / metapyroxenite. They show a flat E-W

**Table 1.** A stratigraphic sequence for Bhavani complex.

Age (Ma)	Group	Major rock type	Era
390 -550	Younger granite	Granite	Proterozoic to Palaeozoic
700 - 900	Ultrabasics / basics younger	Gabbro, Anorthosite	
1600 - 2100	Basic intrusives	Gabbro/Dolerite dyke	Meso Proterozoic
2600	Charnokite group	Charnokite Pyroxene granulite	Late Archaean
3000 - 3100	Mettupalayam complex	Meta-anorthosite Meta-gabbro Meta-pyroxenite Dunite	Archaean
3200	Sathyamangalam group	Amphibolite, basic/ ultrabasic rocks Sillimanite-kyanite-corundum-mica schist Fuchsite-kyanite ferruginous quartzite	Archaean
	Basement	Basement Gneiss	

trending linear bodies showing sub-parallelism to the trend of main shear. The ultramafic and mafic association in the study area shows a dissected pattern and occurs as enclaves within the Peninsular gneisses. Macroscopically, the meta-gabbros are characterized by color indices ranging from approximately 65 to 95 m, with the mafic minerals being dominated by pyroxene, amphibole, and garnet (Rao et al., 1996). Plagioclase feldspar is the dominant light colored mineral in these rocks. Magnetite and ilmenite can also be readily identified in hand sample. The mafic bands meanwhile have an average width of only a couple of millimeters. The weathering makes surface outcrops slightly bumpy, whereas the hand samples tend to be much darker, especially on freshly cut surfaces. The second most litho unit in the present study area is pyroxenite/meta pyroxenite. In Odhimalai, the pyroxenite occurs all along its eastern margin and displays layered contact with metagabbro. In Thenkalmalai the pyroxenite occupies almost half of the hill lock and shears equal proportion whereas in Odhimalai the gabbro is dominant over the pyroxenite. In hand specimen the pyroxenite shows greenish black color along the fringes of outcrop and towards core it becomes darker. Comparing grain size of pyroxenites at both locations are medium to coarse grained. The medium-grained pyroxenites form the important litho unit in the Odhimalai hillock where as the coarse- grained pyroxenites are mostly observed in the Thenkalmalai hillock. In Thenkalmalai area pyroxenite and gabbro shears equal proportion where as in Odhimalai the gabbro is dominant over the pyroxenite (Figure 1). The third most abundant rock type observed in the field area is a meta-anorthositic gabbro, however this lithology is mostly confined to Odhimalai area only and ranges in thickness from 0.5 to 5 m towards the top of hillock. The rocks overall show a granoblastic polygonal

microtexture and display disequilibrium textures (like symplectitic coronas) mostly in metagabbroic rocks containing garnet (Rao et al., 1996). A stratigraphic sequence for the Bhavani complex modified from geological survey of India miscellaneous publication No. 30 is given in Table 1.

## PETROGRAPHY

Petrographic description was performed on 20 thin sections. In hand specimen, the gabbros are dark brownish in colour, whereas the pyroxenites are dark grayish in colour. In thin section gabbros are relatively plagioclase poor (average plagioclase abundances of 10 to 25%) and pyroxene rich. Orthopyroxene is typically coarse grained and is characterized by subhedral crystal surface provided indication of magmatic origin. The plagioclase is mainly equigranular; medium grained and display polygonal texture with angular crystal margins. The plagioclase grains show polysynthetic twinning on albite law. Most of the grains show strain effect in the form of wavy extinction.

Pyroxenites in thin section are texturally characterized by distinct adcumulate texture. They are quite mafic and probably represent pyroxene rich and plagioclase poor portion of cumulate. These pyroxenites are composed of coarse-grained clinopyroxenes, orthopyroxenes and medium grained hornblende crystals. Most of the grains show euhedral crystal surfaces. The accessory phase being the magnetite and ilmenite, concentrated characteristically along the grain boundaries. Clinopyroxenes occur as equigranular coarse euhedral to subhedral grain associated with few interstitial opaques. A few of them exhibit two microtextural features such as exsolution texture and the Fe-Ti oxide rod lets along the

cleavage planes. The coarse grains of clinopyroxenes in pyroxenites display exsolution texture defined by very thin orthopyroxenes with parallel extinction. They are regularly spaced and uniformly distributed throughout the grain, reflecting a compositional gradient across the pyroxene during exsolution. These regularly spaced exsolution lamellae and uniform distribution support the mechanism of exsolution by a homogeneous nucleation and growth in a slowly cooling magmatic system (Buseck et al., 1980) rather than heterogeneous nucleation and growth in which irregular thicker pyroxene exsolution lamellae are developed.

## GEOCHEMISTRY

### Analytical methods

#### *Whole-rock analysis*

Total of sixteen representative samples, seven are pyroxenites and nine are gabbros, were analyzed for bulk chemistry at National Geophysical Research Institute (NGRI) Hyderabad, India. Major elements were determined by X-ray fluorescence Spectrometry (XRF) using Philips MAGIX PRO Model 2440. Trace elements were analyzed by Inductive Coupled Plasma mass Spectroscopy (ICP-MS) using a Perkin Elmer SCIEX ELAN DRC II. The procedure, precision and detection limits are the same as given by Balaram and Rao (2003).

Major, trace, and rare earth element (REEs) data of pyroxenites and gabbros of the Bhavani Complex, Tamil Nadu are given in Table 2. The geochemical signatures of the gabbros and pyroxenites show a significant variation in major and trace elements. The  $\text{SiO}_2$  abundance covers a narrow compositional range in the pyroxenites (49.6-55.5 wt. %) and gabbros (50.1-58 wt. %). The gabbros are characterized by low  $\text{TiO}_2$  (0.26-0.54 wt. %). Whereas the pyroxenites show slightly high concentration of  $\text{TiO}_2$  (0.24-1.7 wt. %).  $\text{MgO}$  content varies from (7.4-13.1 wt. %) in gabbros and (3.6-14.3 wt. %) in pyroxenites. The pyroxenites show high concentration of total iron (8.4-16 wt. %),  $\text{MgO}$  (3.6-14.3 wt. %) with moderate enrichment of  $\text{TiO}_2$  (0.24-1.7 wt. %) and depleted alkalis  $\text{Na}_2\text{O}$  (0.39-2.5 wt. %);  $\text{K}_2\text{O}$  (0.03-1.5 wt. %). The  $\text{CaO-Al}_2\text{O}_3$  relationship of both pyroxenite and gabbro show their trend towards primordial mantle with  $\text{Al}_2\text{O}_3/\text{CaO}$  ratio of  $>1$  in majority of samples (Figure 2). The studied samples have  $\text{CaO}/\text{Al}_2\text{O}_3$  ratios ranging from (0.78-1.8) which is higher as compared to the primordial mantle  $\text{CaO}/\text{Al}_2\text{O}_3$  ratio (0.79) (Hoffmann, 1988). Relative to primordial mantle, the pyroxenites and gabbros show the enriched trend in  $\text{SiO}_2$ ,  $\text{TiO}_2$ , Total iron,  $\text{CaO}$ ,  $\text{Na}_2\text{O}$ , and depleted trend in  $\text{MgO}$  (Table 2). In the alkali- $\text{SiO}_2$  diagram (Figure 3) almost all the samples are broadly classified as gabbro. Bulk composition/whole rock analyses indicate that the magma type is tholeiitic

but trending towards a calc-alkaline nature; this inference is also supported by AFM diagram (after Irvine and Baragar, 1975) (Figure 4). A plot for  $\text{SiO}_2\text{-K}_2\text{O}$  (Figure 5) after Peccerillo and Taylor, 1976) indicates that the samples belong to low-K tholeiitic series. Jensen (1976) cation plot uses  $\text{Al}_2\text{O}_3$ ,  $\text{FeO}^{(t)} + \text{TiO}_2$  and  $\text{MgO}$  cations because of the stability of these elements during metamorphism. The plot (Figure 6) indicates that most of the samples cluster on the border of high-Fe (HFT) and high-Mg (HMT) tholeiitic basalt. Some of the samples are Mg-rich and plot in the basaltic komatiitic (BK) field. The plot again indicates that there is an overall tholeiitic affinity of the magma trending towards a calc-alkaline nature. Based on the  $\text{TiO}_2$ ,  $\text{MnO}$ ,  $\text{P}_2\text{O}_5$  diagram (proposed by Mullen, 1983) most of the studied samples fall within the Calc-alkaline basaltic (CAB) field (Figure 7). Thus it could be inferred that the tectonic environment of eruption is volcanic arc environment and the studied samples fall within the Calc-alkaline basaltic field. Concentration of compatible trace elements in pyroxenites like V (273-309 ppm), Cr (9877-13342 ppm), Co (87-111 ppm) and Ni (676-1055 ppm) are high while these pyroxenites are poor in incompatible and HFS elements like Rb, Hf, Ta, Th, and U. Sr shows a remarkable low concentration ranging from (0.37-0.94 ppm). Similar pattern are observed in gabbro samples being enriched in compatible trace elements and poor in incompatible and HFS elements. Total REE value of pyroxenites varies from 10.13-13.99 ppm with limited REE, ( $\text{Ce}_N/\text{Yb}_N = 0.55\text{-}0.69$ ) and LREE fractionation ( $\text{La}_N/\text{Sm}_N = 1.32\text{-}1.66$ ). The HREE also conclude limited fractionation ( $\text{Gd}_N/\text{Yb}_N = 0.49\text{-}0.58$ ) with negative Eu anomaly. The total REE values of gabbros varies from (12.01-23.48 ppm) with limited REE fractionation ( $\text{Ce}_N/\text{Yb}_N = 0.62\text{-}1.77$ ). LREE ( $\text{La}_N/\text{Sm}_N = 0.54\text{-}1.68$ ) and HREE fractionation is also within limited range ( $\text{Gd}_N/\text{Yb}_N = 1.19\text{-}1.37$ ) with negligible Eu anomaly.

Chondritie-normalized REE plot of the pyroxenites reflects negative Eu anomaly with slight enrichment of HREE (Figure 8). The negative Eu anomaly in these samples may be interpreted as due to fractionation of plagioclase  $\pm$  hornblende and can be imposed when the melt phase enters the stability field of plagioclase. The Low LREE and slight enriched trend of HREE may be due to retention of these elements somewhat by clinopyroxenes or to a greater extent by hornblende. The chondritie-normalized REE plot of gabbros show a flat REE pattern with gentle or without any Eu anomaly (Figure 9). The flat REE pattern in association with low  $\text{CaO}$ ,  $\text{Al}_2\text{O}_3$ , Sr content and absence of Eu anomaly suggests removal of plagioclase component from basic parent magma or may be due to the magma that might have segregated at such depth where plagioclase is not stable and hence it could not be fractionated (Barker et al., 1976). The representative PM and MORB normalized trace element plots for the pyroxenites and gabbros are presented in (Figure 10 and 11a, b). Relative to PM and

**Table 2.** Representative major (wt %) and trace (ppm) element composition of gabbros and pyroxenites from Thenkalmalai and Odhimalai (Mettupailium Ultramafic complex), Tamilnadu, Southern India.

Rock type	Gabbro																Pyroxenite																PM*	
Sample No	OM-06	OM-07	OM-08	OM-13	OM-22	OM-23	OM-25	OM-33	OM-48	OM-32	OM-37	OM-38	OM-39	OM-40	OM-45	OM-52	OM-06	OM-07	OM-08	OM-13	OM-22	OM-23	OM-25	OM-33	OM-48	OM-32	OM-37	OM-38	OM-39	OM-40	OM-45	OM-52		
SiO <sub>2</sub>	51.5	52.3	50.1	51.5	58	53.5	54	54	49.9	55.5	51.8	52.6	51.4	51.8	49.6	53.9	45.96	51.5	58	53.5	54	49.9	55.5	51.8	52.6	51.4	51.8	49.6	53.9	45.96				
TiO <sub>2</sub>	0.36	0.41	0.35	0.37	0.32	0.3	0.26	0.39	0.54	0.88	0.65	0.24	1.7	0.42	0.58	0.45	0.18	0.36	0.41	0.35	0.37	0.32	0.3	0.26	0.39	0.54	0.88	0.65	0.24	1.7	0.42	0.58	0.45	0.18
Al <sub>2</sub> O <sub>3</sub>	11.0	12.8	9.4	9.7	9.9	12.4	11.5	12	13	13.1	13.6	8.4	10.6	13.7	13	6	4.06	11.0	12.8	9.4	9.7	9.9	12.4	11.5	12	13	13.1	13.6	8.4	10.6	13.7	13	6	4.06
Fe <sub>2</sub> O <sub>3</sub>	10.4	10.7	16.9	16.2	11.2	11.4	15	10.3	13.9	13.5	16	8.4	15.4	11.8	12.6	15.8	7.54	10.4	10.7	16.9	16.2	11.2	11.4	15	10.3	13.9	13.5	16	8.4	15.4	11.8	12.6	15.8	7.54
MnO	0.16	0.15	0.25	0.16	0.12	0.13	0.12	0.13	0.18	0.19	0.21	0.11	0.19	0.17	0.13	0.23	0	0.16	0.15	0.25	0.16	0.12	0.13	0.12	0.13	0.18	0.19	0.21	0.11	0.19	0.17	0.13	0.23	0
MgO	11.9	10.0	13.1	10.2	11.1	11.3	7.4	12.1	9	3.6	6.5	14.3	6.6	8	10.3	7.9	37.78	11.9	10.0	13.1	10.2	11.1	11.3	7.4	12.1	9	3.6	6.5	14.3	6.6	8	10.3	7.9	37.78
CaO	13.4	12.2	9	10.6	8.7	10.4	11.2	10.4	12.1	10.9	8.4	15.5	12.6	12.7	10.3	15.1	3.21	13.4	12.2	9	10.6	8.7	10.4	11.2	10.4	12.1	10.9	8.4	15.5	12.6	12.7	10.3	15.1	3.21
Na <sub>2</sub> O	1.1	1.3	0.76	1	0.41	0.41	0.41	0.55	1.3	1.9	2.5	0.39	1.2	1.2	1.7	0.53	0.33	1.1	1.3	0.76	1	0.41	0.41	0.41	0.55	1.3	1.9	2.5	0.39	1.2	1.2	1.7	0.53	0.33
K <sub>2</sub> O	0.08	0.11	0.10	0.20	0.08	0.07	0.08	0.11	0.06	0.32	0.13	0.05	0.24	0.09	1.5	0.03	0	0.08	0.11	0.10	0.20	0.08	0.07	0.08	0.11	0.06	0.32	0.13	0.05	0.24	0.09	1.5	0.03	0
P <sub>2</sub> O <sub>5</sub>	0.02	0.03	0.02	0.03	0.01	0.02	0.01	0.01	0.03	0.07	0.08	0.01	0.06	0.03	0.24	0.02	0	0.02	0.03	0.02	0.03	0.01	0.02	0.01	0.01	0.03	0.07	0.08	0.01	0.06	0.03	0.24	0.02	0
<b>Total</b>	<b>9.92</b>	<b>100</b>	<b>99.98</b>	<b>99.96</b>	<b>9.84</b>	<b>99.93</b>	<b>99.98</b>	<b>100</b>	<b>99.96</b>	<b>99.87</b>	<b>100</b>	<b>99.99</b>	<b>99.91</b>	<b>99.95</b>	<b>99.96</b>	<b>99.06</b>	<b>99.99</b>	<b>9.92</b>	<b>100</b>	<b>99.98</b>	<b>99.96</b>	<b>9.84</b>	<b>99.93</b>	<b>99.98</b>	<b>100</b>	<b>99.96</b>	<b>99.87</b>	<b>100</b>	<b>99.99</b>	<b>99.91</b>	<b>99.95</b>	<b>99.96</b>	<b>99.06</b>	<b>99.99</b>
Sc (ppm)	44.9	43.2	45.7	47.3	45.6	52.5	46.5	47.3	46.8	9.9	8.9	8.6	7.7	8.5	8	7.9		44.9	43.2	45.7	47.3	45.6	52.5	46.5	47.3	46.8	9.9	8.9	8.6	7.7	8.5	8	7.9	
V	195.2	205.5	219.3	235.3	304.1	180.2	222.3	260.5	242.7	298.6	286.5	288.3	263	307.7	309.4	273.7		195.2	205.5	219.3	235.3	304.1	180.2	222.3	260.5	242.7	298.6	286.5	288.3	263	307.7	309.4	273.7	
Cr	957.6	1683.2	1240.3	1188.4	82.6	2291.9	12007.5	546.1	778.9	21200.4	10690.4	12720.9	13342.2	11503	11938	9877.1		957.6	1683.2	1240.3	1188.4	82.6	2291.9	12007.5	546.1	778.9	21200.4	10690.4	12720.9	13342.2	11503	11938	9877.1	
Co	44.6	75.7	53	54.3	49.6	57.3	53.2	55.8	49.5	111.5	102.5	108.7	104.4	106.1	94.1	87.1		44.6	75.7	53	54.3	49.6	57.3	53.2	55.8	49.5	111.5	102.5	108.7	104.4	106.1	94.1	87.1	
Ni	188.6	249.4	196.7	186	81.6	305	192	151.7	163.3	1055.4	894.5	1016.5	990.5	851.3	676.8	1013.4		188.6	249.4	196.7	186	81.6	305	192	151.7	163.3	1055.4	894.5	1016.5	990.5	851.3	676.8	1013.4	
Cu	35.3	33.9	23.7	26.9	21.4	19.1	39.9	34.5	30.2	60.7	66.3	59	115.7	34.8	90.2	78		35.3	33.9	23.7	26.9	21.4	19.1	39.9	34.5	30.2	60.7	66.3	59	115.7	34.8	90.2	78	
Zn	42.8	51.0	38.7	50.4	45.9	52.3	66.7	51.7	53	72.3	57.4	73.8	83	59.4	64.2	46.6		42.8	51.0	38.7	50.4	45.9	52.3	66.7	51.7	53	72.3	57.4	73.8	83	59.4	64.2	46.6	
Rb	1.7	2.5	3.5	1.4	1.4	1.6	1.5	1.5	2.8	16.4	9.7	4.4	6	4.3	11.2	5.5		1.7	2.5	3.5	1.4	1.4	1.6	1.5	1.5	2.8	16.4	9.7	4.4	6	4.3	11.2	5.5	
Sr	6.3	4.8	4.6	5.2	4.9	1.4	4.6	4.1	2	0.57	0.71	0.44	0.53	0.37	0.39	0.94		6.3	4.8	4.6	5.2	4.9	1.4	4.6	4.1	2	0.57	0.71	0.44	0.53	0.37	0.39	0.94	
Y	0.33	0.30	0.36	0.42	0.53	0.27	0.40	0.50	0.5	1.9	2.2	2.1	1.7	2.2	2.4	2.1		0.33	0.30	0.36	0.42	0.53	0.27	0.40	0.50	0.5	1.9	2.2	2.1	1.7	2.2	2.4	2.1	
Zr	0.12	0.11	0.17	0.16	0.11	0.16	0.15	0.15	0.16	0.27	0.32	0.27	0.24	0.37	0.3	0.28		0.12	0.11	0.17	0.16	0.11	0.16	0.15	0.15	0.16	0.27	0.32	0.27	0.24	0.37	0.3	0.28	
Nb	0.25	0.42	0.31	0.28	0.75	0.22	0.35	0.25	0.34	3.7	4.4	4.3	4.3	4.7	4.8	4.8		0.25	0.42	0.31	0.28	0.75	0.22	0.35	0.25	0.34	3.7	4.4	4.3	4.3	4.7	4.8	4.8	
Ba	18.7	6.7	4.9	3.9	7.7	4.0	4.4	3.1	5.2	19.6	6.6	8	5.8	6.8	7	8.2		18.7	6.7	4.9	3.9	7.7	4.0	4.4	3.1	5.2	19.6	6.6	8	5.8	6.8	7	8.2	
Hf	0.18	0.14	0.22	0.21	0.23	0.18	0.22	0.22	0.24	0.42	0.43	0.45	0.36	0.55	0.49	0.46		0.18	0.14	0.22	0.21	0.23	0.18	0.22	0.22	0.24	0.42	0.43	0.45	0.36	0.55	0.49	0.46	
Ta	0.04	0.07	0.04	0.04	0.10	0.03	0.05	0.03	0.04	0.01	0.04	0.05	0.08	0.02	0.02	0.15		0.04	0.07	0.04	0.04	0.10	0.03	0.05	0.03	0.04	0.01	0.04	0.05	0.08	0.02	0.02	0.15	
Th	0.17	0.22	0.07	0.07	0.07	0.09	0.09	0.07	0.13	1.3	1.2	1.5	1.03	1.2	0.72	2.7		0.17	0.22	0.07	0.07	0.07	0.09	0.09	0.07	0.13	1.3	1.2	1.5	1.03	1.2	0.72	2.7	
U	0.09	0.07	0.05	0.0	0.12	0.19	0.15	0.11	0.18	0.13	0.05	0.21	0.1	0.08	0.1	0.25		0.09	0.07	0.05	0.0	0.12	0.19	0.15	0.11	0.18	0.13	0.05	0.21	0.1	0.08	0.1	0.25	
La	2.53	1.63	1.48	1.35	2.50	1.37	1.26	0.93	1.21	1.16	1.02	1.28	0.83	1.30	1.05	1.15		2.53	1.63	1.48	1.35	2.50	1.37	1.26	0.93	1.21	1.16	1.02	1.28	0.83	1.30	1.05	1.15	
Ce	4.46	3.88	3.74	3.34	5.62	2.83	3.17	2.33	2.92	2.93	2.91	2.94	2.26	3.40	3.08	2.88		4.46	3.88	3.74	3.34	5.62	2.83	3.17	2.33	2.92	2.93	2.91	2.94	2.26	3.40	3.08	2.88	
Pr	0.56	0.56	0.53	0.48	0.82	0.42	0.54	0.42	0.47	0.34	0.34	0.37	0.28	0.38	0.39	0.36		0.56	0.56	0.53	0.48	0.82	0.42	0.54	0.42	0.47	0.34	0.34	0.37	0.28	0.38	0.39	0.36	
Nd	3.01	3.23	2.89	2.85	4.95	2.50	3.34	2.86	3.14	1.71	1.91	1.83	1.46	1.94	2.08	1.82		3.01	3.23	2.89	2.85	4.95	2.50	3.34	2.86	3.14	1.71	1.91	1.83	1.46	1.94	2.08	1.82	
Sm	0.94	0.89	0.86	0.92	1.49	0.74	1.06	1.06	1.08	0.44	0.48	0.45	0.38	0.50	0.52	0.45		0.94	0.89	0.86	0.92	1.49	0.74	1.06	1.06	1.08	0.44	0.48	0.45	0.38	0.50	0.52	0.45	

Table 2. Contd

Eu	0.37	0.30	0.33	0.38	0.59	0.26	0.36	0.41	0.37	0.12	0.13	0.12	0.11	0.14	0.14	0.12
Gd	1.18	1.01	1.03	1.28	1.75	0.87	1.21	1.40	1.46	0.79	0.85	0.89	0.67	0.89	0.95	0.89
Tb	0.20	0.16	0.19	0.23	0.29	0.16	0.21	0.27	0.27	0.16	0.17	0.18	0.14	0.20	0.20	0.18
Dy	1.54	1.24	1.45	1.80	2.20	1.18	1.66	2.12	2.01	1.38	1.48	1.49	1.18	1.55	1.71	1.49
Ho	0.35	0.27	0.32	0.39	0.50	0.26	0.36	0.48	0.47	0.35	0.38	0.37	0.31	0.39	0.44	0.38
Er	0.98	0.79	0.90	1.10	1.32	0.71	1.01	1.31	1.29	1.12	1.26	1.21	1.02	1.28	1.43	1.26
Tm	0.13	0.10	0.12	0.14	0.17	0.09	0.13	0.17	0.16	0.18	0.21	0.19	0.17	0.20	0.23	0.20
Yb	0.76	0.59	0.71	0.81	1.05	0.51	0.76	1.01	0.98	1.20	1.42	1.26	1.13	1.33	1.51	1.31
Lu	0.16	0.13	0.16	0.18	0.23	0.11	0.17	0.22	0.22	0.21	0.25	0.24	0.20	0.25	0.26	0.23
Pb	6.08	5.9	6.10	4.20	5.17	4.71	5.19	5.29	5.96	0.01	0.02	0.01	0.02	0.01	0.01	0.01
$\Sigma$ REEs	17.17	14.78	14.71	12.25	23.48	12.01	15.24	14.99	16.05	12.08	12.81	12.83	10.13	13.75	13.99	12.73
Ce <sub>N</sub> /Yb <sub>N</sub>	1.58	1.77	1.42	1.11	1.44	1.49	1.13	0.62	0.80	0.66	0.55	0.63	0.54	0.69	0.55	0.59
La <sub>N</sub> /Sm <sub>N</sub>	1.68	1.14	1.07	0.91	1.04	1.15	0.74	0.54	0.70	1.66	1.32	1.76	1.35	1.62	1.25	1.58
Gd <sub>N</sub> /Yb <sub>N</sub>	1.28	1.41	1.19	1.30	1.37	1.41	1.31	1.14	1.23	0.54	0.49	0.58	0.49	0.55	0.52	0.56
Eu/Eu*	1.06	0.96	1.06	1.06	1.11	.98	0.96	1.02	0.89	0.62	0.61	0.57	0.65	0.63	0.60	0.57
Rb/Nb	7.51	6.69	12.69	5.76	2.14	8.03	4.71	6.65	9.31	4.97	2.48	1.14	1.54	1.03	2.64	1.27
Th/Nb	5.71	4.38	1.90	2.10	0.78	3.41	2.16	2.34	3.18	2.95	2.24	2.91	1.98	2.15	1.26	4.67

PM\* = Primordial mantle major oxides data after Hofmann (1988). Fe<sub>2</sub>O<sub>3</sub><sup>1</sup> = Total iron as Fe<sub>2</sub>O<sub>3</sub>.

MORB, both set of rocks show enrichment of LILEs and LREEs. They are further characterized by a low Th abundance and a distinct Nb-Ta, Zr-Hf troughs.

These features are characteristic of tholeiitic basalts produced at destructive plate margins or within plate tholeiites which are contaminated by continental crust (Hawkesworth et al., 1994). The depletion of Nb is not affected by the fractional crystallization and it is known that Nb anomaly in modern arc volcanic is independent of the degree of crystallization.

Since the Nb is not transferable into slab, the depletion of Nb is thought to reflect formation in supra-subduction zone tectonic setting (Brique and Joron, 1984).

## PETROGENESIS

The whole-rock chemical data can provide useful information on the course of fractional crystallization/magmatic evolution. The various binary diagrams (Figure 12) have been plotted in order to evaluate the evolution of the studied samples. The MgO has been taken as the reference value because of its wide range and plays an important role in process of fractional crystallization. The studied samples show increasing trend of SiO<sub>2</sub>, K<sub>2</sub>O+ Na<sub>2</sub>O, Fe<sub>2</sub>O<sub>3</sub> and TiO<sub>2</sub> with the decrease of MgO whereas CaO and CaO/Al<sub>2</sub>O<sub>3</sub> show decreasing trend with the decrease of MgO. A positive correlation observed between CaO, CaO/Al<sub>2</sub>O<sub>3</sub> and MgO supports the

fractionation of clinopyroxenes. During the plagioclase removal, CaO/Al<sub>2</sub>O<sub>3</sub> ratio increases whereas it remains constant during olivine fractionation (Dungan and Rnodes, 1978). Thus it could be inferred that the high value of CaO/Al<sub>2</sub>O<sub>3</sub> ratio (greater than 0.8) in the studied samples may be due to plagioclase fractionation. Fractional crystallization associated with crustal contamination is an important process during magmatic evolution (De-Paolo, 1981) and may modify both elemental and isotopic compositions. Crustal materials are rich in LILEs, K<sub>2</sub>O and Na<sub>2</sub>O and depleted in P<sub>2</sub>O<sub>5</sub> and TiO<sub>2</sub>. Low concentration and narrow range of K<sub>2</sub>O and Na<sub>2</sub>O in the investigated samples suggests in favor of their minimal crustal contamination.

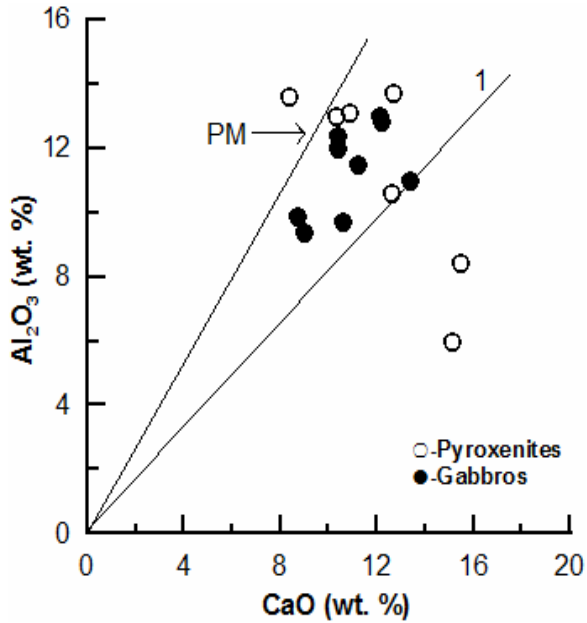


**Figure 2.** CaO vs Al<sub>2</sub>O<sub>3</sub> diagram depicts that the CaO content of gabbros and pyroxenites tends to be close to primordial mantle array (Hoffman, 1988).

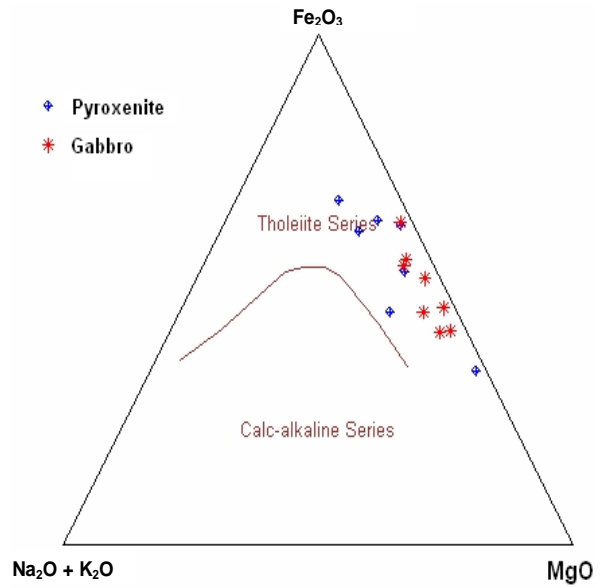


**Figure 4.** AFM diagram for gabbros and pyroxenites (after Irvine and Baragar, 1975).

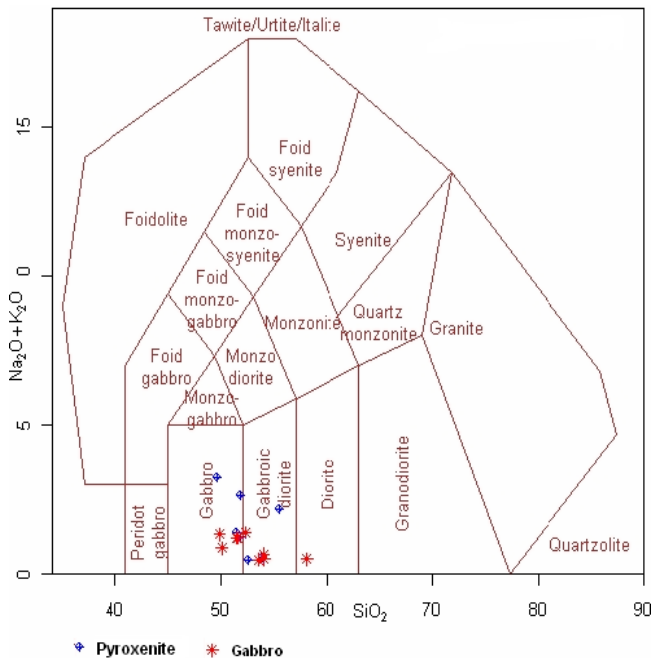


**Figure 3.** Rock classification diagram (Total alkali Vs SiO<sub>2</sub>) after Middlemost (1985).

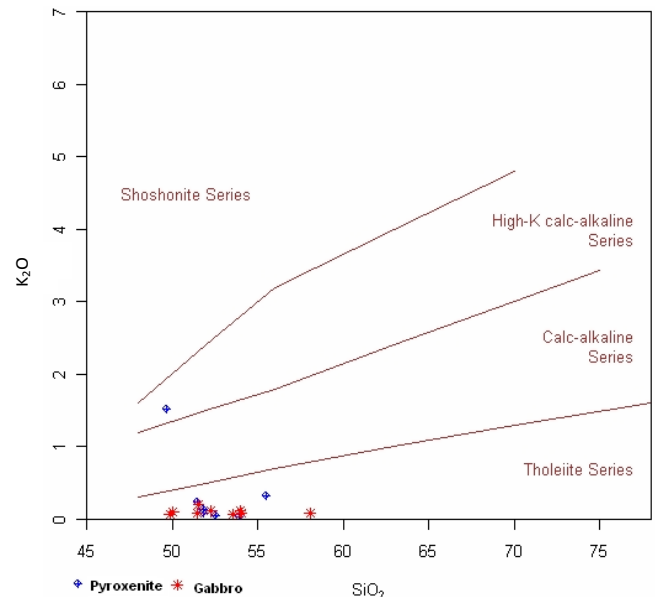


**Figure 5.** Rock classification diagram (K<sub>2</sub>O vs SiO<sub>2</sub> after Peccerilli and Taylor 1976).

The values of Nb/La and Nb/Ce of the studied samples show that the gabbros have a quite low range of Nb/La and Nb/Ce (0.09-0.3) and (0.05- 0.13), where as the pyroxenites show slightly high range of Nb/La (3.18-5.24)

and Nb/Ce (1.25-1.92) respectively. These values for gabbros are not only very low compared to those of primitive mantle (PM 1.02 and 0.40, respectively, Taylor and McLennan, 1985; 1.04 and .40, respectively, Sun and McDonough, 1989) but are also lower than the average bulk crust (0.69 and 0.33 respectively). Such lower values are not expected to be produced by processes of contamination by an average crustal

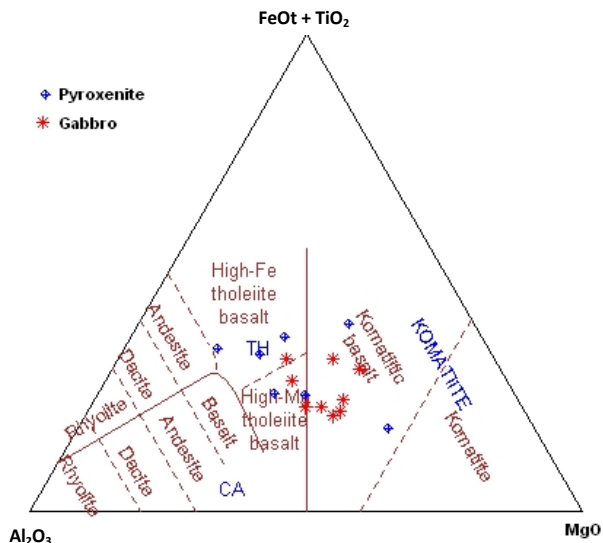


Figure 6. Jensen's cation Plot for gabbros and pyroxenites (after Jensen 1976).

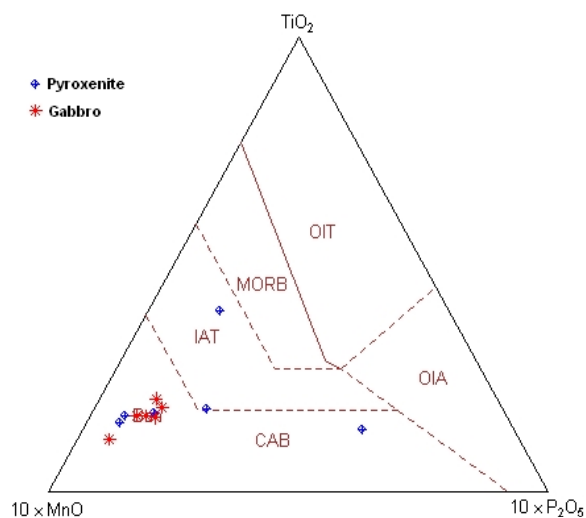


Figure 7. TiO<sub>2</sub>-MnO-P<sub>2</sub>O<sub>5</sub> triplot for gabbros and pyroxenites (after Mullen 1983).

component. Thus, it can be inferred that these trace element characteristics may have been obtained by studied rocks due to LREEs-LILEs enriched source characteristics with depletion of high field strength elements (such as Nb) at plate margin settings (Weaver and Tarney, 1983; Ahmad and Tarney, 1994; Mir et al., 2011, 2013). Enrichment of LILEs and depletion of HFSEs may also occur in within plate tectonic setting rocks due to crustal contamination, but, studied rocks show least crustal contamination. The geochemistry of mafic and ultramafic rocks is most commonly used to discriminate tectonic setting.

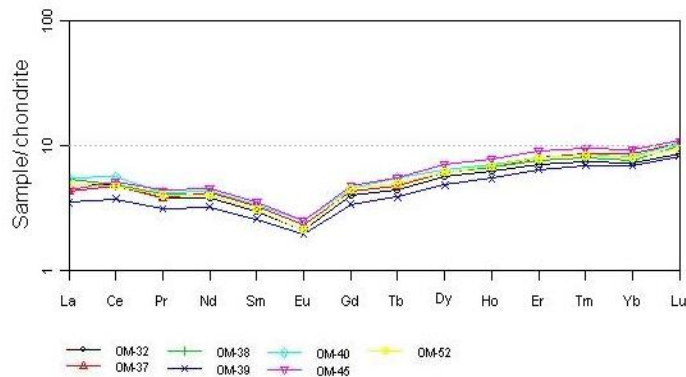


Figure 8. Chondrite normalized REE diagram for the pyroxenites after Sun and McDonough (1989).

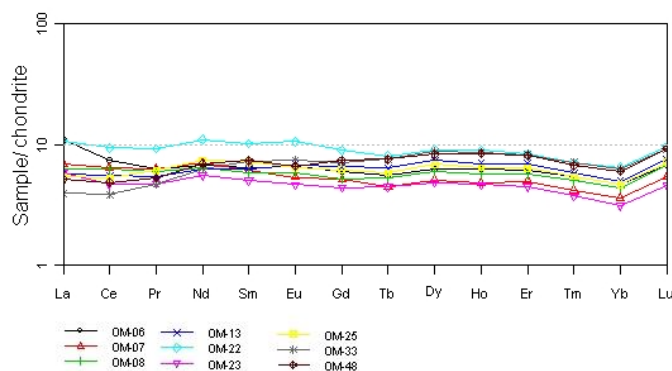
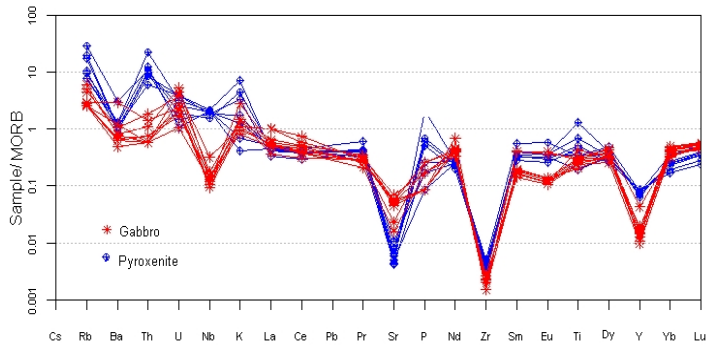


Figure 9. Chondrite normalized REEs diagram for the gabbros from Bhavani ultramafic complex normalized after Sun and McDonough (1989).

According to Pearce and Cann (1973) it is possible to use geochemistry to distinguish between basalts produced in different known tectonic settings. The basaltic rocks are formed in almost every tectonic environment and they are believed to be geochemically sensitive to the changes in plate tectonic frame work. In order to understand the tectonic environment of the studied samples the plot Ti/1000 vs. V (after Shervais, 1982) shown in Figure 13 depicts that the studied samples fall in the Arc tholeiitic environment. To support this, tri-plot proposed by Mullen (1983). Figure 6 shows that the majority of the samples fall in the calcic-alkaline basaltic field of arc environment. In addition, geochemical ratios such as La/Yb and La/Sm are good indicators of mantle sources and degree of melting (Verma, 2006; Mir et al., 2011). Rift rocks show high (La/Yb)<sub>cn</sub> and (La/Sm)<sub>cn</sub> values, whereas arc/back arc show low values of both parameters (Verma, 2006). Therefore the low values of both parameters (La/Yb)<sub>cn</sub> < 2.31 and (La/Sm)<sub>cn</sub> < 1.76 in the studied samples may indicate the volcanic arc setting.





**Figure 10.** MORB normalized diagram for gabbros and pyroxenites after Sun and McDonough (1989).

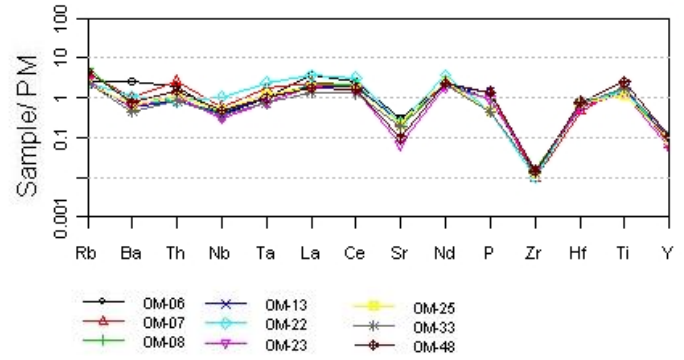


**Figure 11b.** Primitive element-normalized multi-element diagram for gabbros after Sun and McDonough (1989).

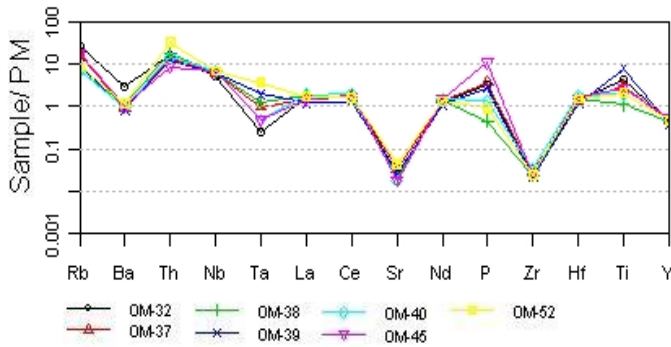


**Figure 11a.** Primitive element-normalized multi-element diagram for pyroxenites after Sun and McDonough (1989).

**CONCLUSIONS**

On the alkali-SiO<sub>2</sub> diagram almost all the studied samples are broadly classified as gabbros. On the bases of relationship among major oxides such as SiO<sub>2</sub>, K<sub>2</sub>O, Al<sub>2</sub>O<sub>3</sub>, FeO(t), TiO<sub>2</sub> and MgO magma type of studied samples is tholeiitic in nature, however, based on the TiO<sub>2</sub>, MnO, P<sub>2</sub>O<sub>5</sub> diagram most of the studied samples fall within the calc-alkaline basaltic (CAB) field. Thus it could be inferred that the tectonic environment of eruption is volcanic arc environment. Low concentration and narrow range of K<sub>2</sub>O and Na<sub>2</sub>O in the investigated samples suggests in favor of their least crustal contamination. Low values of Nb/La and Nb/Ce in studied gabbros also discourages the crustal contamination. The negative Eu anomaly in pyroxenites depicts fractionation of plagioclase. The Low LREEs and slight enriched trend of HREEs may be due to retention of these elements somewhat by clinopyroxenes or to a greater extent by hornblende. The chondritic normalized REEs plot of gabbros show a flat REEs pattern with gentle or without

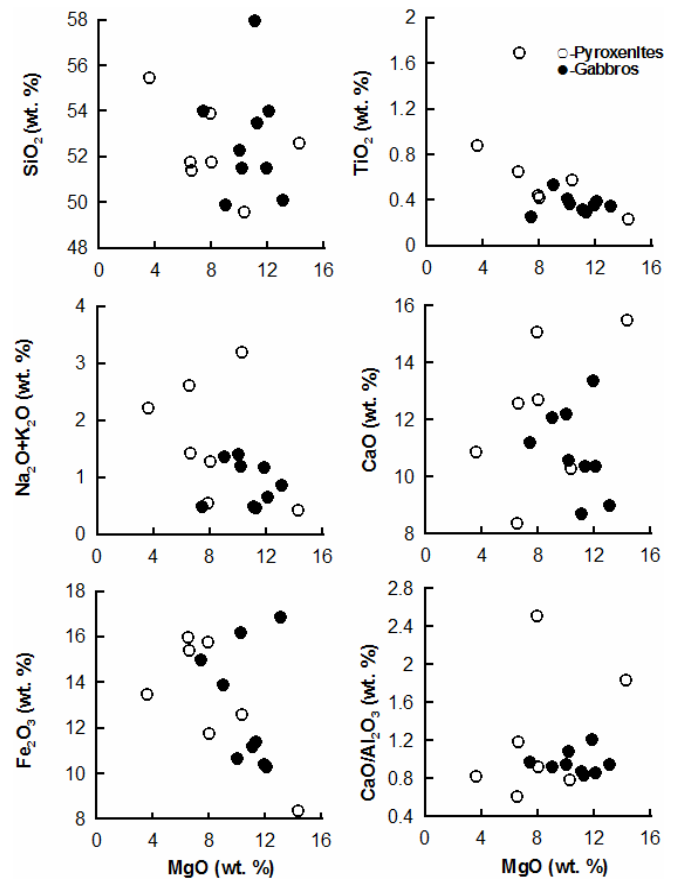


**Figure 12.** Binary plots of gabbros and pyroxenites: MgO Vs, SiO<sub>2</sub>, : MgO Vs Na<sub>2</sub>O+K<sub>2</sub>O, : MgO Vs Fe<sub>2</sub>O<sub>3</sub>, : MgO Vs TiO<sub>2</sub>, : MgO Vs CaO, : MgO Vs CaO/Al<sub>2</sub>O<sub>3</sub>.

any Eu anomaly. The flat REEs pattern in association with low CaO, Al<sub>2</sub>O<sub>3</sub>, Sr content and absence of Eu anomaly suggests removal of plagioclase component from basic parent magma. In addition to tectonic setting discrimination diagrams their geochemical characteristics

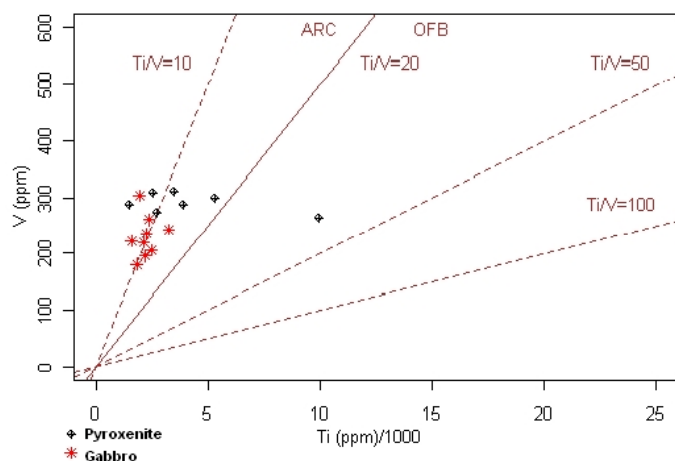


**Figure 13.** Ti/1000 Vs V tectonic discrimination diagram (after Shervais 1982) for gabbros and pyroxenites.

such as low Th abundance, significant Nb-Ta and Zr-Hf anomalies, low values of  $(La/Yb)_{cn}$  and  $(La/Sm)_{cn}$  favours the inference of arc tectonic setting of these rocks.

### Conflict of Interests

The author(s) have not declared any conflict of interests.

### REFERENCES

- Ahmad T, Tarney J (1994). Geochemistry and petrogenesis of late Archean Aravalli volcanic, basement enclaves and granitoids, Rajasthan. *Precamb. Res.* 65:1-23. [http://dx.doi.org/10.1016/0301-9268\(94\)90097-3](http://dx.doi.org/10.1016/0301-9268(94)90097-3)
- Balaram V, Rao TG (2003). Rapid determination of REE and other trace elements in geological samples by microwave acid digestion and ICP-MS. *Atom. Spectrosc.* 24:206-212.
- Barker F, Arth JG, Peterman ZE, Friedman I (1976). The 1.7 to 1.8-b.y. old trondhiemites of south western Colorado and northern new mexico. *Geochemistry and depth of genesis.* *Geol. Soc. Am. Bull.* 87:189-189. [http://dx.doi.org/10.1130/0016-7606\(1976\)87<189:TTBTOS>2.0.CO;2](http://dx.doi.org/10.1130/0016-7606(1976)87<189:TTBTOS>2.0.CO;2)
- Bhaskar Rao YJ, Chetty TRK, Janardhan AS, Gopalan K (1996). Sm-Nd and Rb-Sr ages and P-T history of the Archean Sittampundi and Bhavani layered meta-anorthosite complexes in Cauvery shear zone, South India: evidence for Neoproterozoic reworking of Archean crust. *Contrib. Mineral. Petrol.* 125: 237-250. <http://dx.doi.org/10.1007/s004100050219>
- Brique L, Bougault Joron JL (1984). Quantification of Nb, Ta, Ti, and V anomalies in magmas associated with Subduction zones: petrogenetic implication. *Earth Planet. Sci. Lett.* 68:297-308. [http://dx.doi.org/10.1016/0012-821X\(84\)90161-4](http://dx.doi.org/10.1016/0012-821X(84)90161-4)
- De-Paolo DJ (1981). Trace element and isotopic effects of combined wallrock assimilation and fractional crystallization. *Earth Planet. Sci. Lett.* 53:189-202. [http://dx.doi.org/10.1016/0012-821X\(81\)90153-9](http://dx.doi.org/10.1016/0012-821X(81)90153-9)
- Dungan MA, Rnodes JM (1978). Residual glasses and melt inclusions in basalts from DSDP Legs 45 and 46: evidence for magma mixing. *Contrib. Mineral. Petrol.* 67:417-431. <http://dx.doi.org/10.1007/BF00383301>
- Hawkesworth CJ, Gallagher AK, Hergt JM, Mcdermott BF (1994). Destructive plate margin magmatism: Geochemistry and melt generation. *Lithos* 33:169-188. [http://dx.doi.org/10.1016/0024-4937\(94\)90059-0](http://dx.doi.org/10.1016/0024-4937(94)90059-0)
- Hoffmann AW (1988). Chemical differentiation of the earth: the relationship between mantle, continental crust and oceanic crust. *Earth planet. Sci. Lett.* 90:297-314. [http://dx.doi.org/10.1016/0012-821X\(88\)90132-X](http://dx.doi.org/10.1016/0012-821X(88)90132-X)
- Irvine TA, Baragar WRA (1975). A guide to the chemical classification of the common volcanic rocks. *Canad. J. Earth Sci.* 8:523-546. <http://dx.doi.org/10.1139/e71-055>
- Jensen LS (1976). A new cation plot for classifying subalkalic volcanic rocks. *Min. Nat. Resources Ontario Division of Mines Misc paper* 66:20.
- Middlemost EAK (1985). Naming materials in the magma/igneous rock system. *Earth-Sciences Reviews* 37:215-224. [http://dx.doi.org/10.1016/0012-8252\(94\)90029-9](http://dx.doi.org/10.1016/0012-8252(94)90029-9)
- Mir AR, Alvi SH, Balaram V (2011). Geochemistry of the mafic dykes in parts of the Singhbhum Granitoid complex: petrogenesis and tectonic setting. *Arab. J. Geos.* 4:933-943. <http://dx.doi.org/10.1007/s12517-010-0121-6>
- Mir AR, Alvi SH, Balaram V, Bhat FA, Sumira Z, Dar SA (2013). A subduction zone geochemical characteristic of the newer dolerite dykes in the Singhbhum craton, Eastern India. *Inter. Res. J. Geol. Min.* 3:213-223.
- Mullen ED (1983). MnO/TiO<sub>2</sub>/P<sub>2</sub>O<sub>5</sub>: a minor element discriminant for basaltic rocks of oceanic environments and its implications for petrogenesis. *Earth Planet. Sci. Lett.* 62:53-62. [http://dx.doi.org/10.1016/0012-821X\(83\)90070-5](http://dx.doi.org/10.1016/0012-821X(83)90070-5)
- Pearce JA, Cann JR (1973). Tectonic setting of basic volcanic rocks determined using trace element analyses. *Earth Planet. Sci. Lett.* 19:290-300. [http://dx.doi.org/10.1016/0012-821X\(73\)90129-5](http://dx.doi.org/10.1016/0012-821X(73)90129-5)
- Peccerillo A, Taylor SR (1976). Geochemistry of Eocene calc-alkaline volcanic rocks from the Kastamonu area, Northern Turkey. *Contrib. Mineral. Petrol.* 58:63-81. <http://dx.doi.org/10.1007/BF00384745>
- Rao YJB, Chetty TRK, Janardhan AS, Gopalan K (1996). Sm-Nd and Rb-Sr ages and P-T history of the Archean Sittampundi and Bhavani layered meta-anorthosite complexes in Cauvery shear zone, South India: evidence for Neoproterozoic reworking of Archean crust. *Contrib. Mineral. Petrol.* 125: 237-250. <http://dx.doi.org/10.1007/s004100050219>
- Selvan TA (1981). Anorthosite-gabbro-ultramafic complex around Gobichettypalayam, Tamil Nadu and their possible relation to Sittampundi type anorthosite complex (unpublished). Ph.D. thesis Univ Mysore Mysore India.
- Shervais JW (1982). Ti-V Plots and Petrogenesis of modern and ophiolitic Lavas. *Earth Planet. Sci. Lett.* 59: 108-118. [http://dx.doi.org/10.1016/0012-821X\(82\)90120-0](http://dx.doi.org/10.1016/0012-821X(82)90120-0)
- Sun S, McDonough WF (1989). Chemical and isotopic systematic of oceanic basalts: implications for mantle composition and processes. In: Saunders AD, Norry MJ (Eds), *Magmatism in the ocean basins.* *Geol. Soc. London Sp. Pub.* 42:313-345.
- Subramanian KS, Selvan TA (2001). *Geology of Tamil Nadu and Pondicherry.* *Geol. Soc. India (Text-book series).* P. 192.
- Taylor SR, McLennan SM (1985). *The continental crust: its composition and evolution.* Blackwell, Oxford.
- Verma SP (2006). Extension-related origin of magmas from a garnet-bearing source in the Los Tuxtlas volcanic field, Mexico. *Int. J. Earth Sci. (Geol Rundsch)* 95:871-901. <http://dx.doi.org/10.1007/s00531-006-0072-z>
- Weaver BL, Tarney J (1983). Chemistry of the sub continental mantle inferences from Archean and Proterozoic dykes and continental flood basalts. In: Hawkesworth CJ, Norry MJ (eds) *Continental Basalt and Mantle Xenoliths.* Shiva Nantwich: pp. 209-229.